Systematic Study on Structural Phase Behavior of CdSe Thin Films

ARTICLE *in* THE JOURNAL OF PHYSICAL CHEMISTRY B · DECEMBER 2005

Impact Factor: 3.3 · DOI: 10.1021/jp053124c · Source: PubMed

2 AUTHORS:

Rohidas B. Kale
The Institute of Science, Mumbai
25 PUBLICATIONS **607** CITATIONS
SEE PROFILE

Dayanand Lokhande
Solapur University
17 PUBLICATIONS **370** CITATIONS
SEE PROFILE

Systematic Study on Structural Phase Behavior of CdSe Thin Films

R. B. Kale*,† and C. D. Lokhande‡

Department of Physics, Rajaram College (Government of Maharashtra), Kolhapur-416004, India, and Thin Film Physics Laboratory, Department of Physics, Shivaji University, Kolhapur-416004, India

Received: June 10, 2005; In Final Form: August 14, 2005

Cadmium selenide (CdSe) thin films were chemically deposited at room temperature, from aqueous ammoniacal solution using $Cd(CH_3COO)_2$ as Cd^{2+} and Na_2SeSO_3 as Se^{2-} ion sources. The as-deposited films were uniform, well adherent to the glass substrate, specularly reflective, and red-orange in color. The as-deposited CdSe layers grew with nanocrystalline sphalerite cubic structure along with the amorphous phase present in it, with optical band gap $E_g = 2.3$ eV. The films were annealed in air atmosphere for 4 h at different temperatures and characterized for compositional, structural, morphological, and optical properties. XRD and SEM studies clearly revealed the systematic phase transformation of CdSe films from metastable nanocrystalline cubic (zinc blende type) to a mixture of cubic and hexagonal (wurtzite type), and finally into stable hexagonal through different intermediate phases with an improvement in the crystal quality. The films showed a red shift in their optical spectra after annealing.

1. Introduction

Semiconductor nanoparticles have attracted widespread attention because of their size-dependent structural, morphological, optical, and electronic properties arising from the quantum confinement of electrons and large surface-to-volume ratio of nanoparticles.[1−6] Among these, CdSe (E_g, bulk = 1.7 eV, group II−VI) nanoparticles have received considerable attention because of their tunable band gap, which can vary their optical response from the infrared region to the ultraviolet, and their major contribution to solar cells, photoelectronics, light amplifiers, thin film transistors and single-electron transistors, light-emitting diodes, and lasers.[7] Among the various applications, cadmium selenide has been studied intensively in recent years as a photoanode in photoelectrochemical (PEC) cells.[8] The conversion efficiency of these cells as well as the physicochemical stability of the anode in an electrolyte system depends critically on the structure and composition of the CdSe films. An essential criterion for obtaining high efficiency from PEC cells is the use of the CdSe photoanode as a thin film with large crystallites in preferably a hexagonal crystalline phase. The larger crystallites inhibit photocarrier losses due to grain boundary recombination, and the hexagonal phase has a higher photoabsorbance and provides much needed stability against corrosive electrolyte in PEC cells.[9] Among various other methods, the chemical bath deposition (CBD) method is found to be an inexpensive, simple, and convenient method for depositing large area nanocrystalline thin films at relatively low temperatures. A number of researchers have deposited CdSe thin films using the CBD method and reported different types of crystal structures, i.e., amorphous,[10−12] cubic,[2,13] a mixture of cubic and hexagonal,[14,15] and hexagonal.[16,17] Thus structural phases and properties of CdSe films prepared by the CBD method were critically dependent on various preparative parameters such as the sources and concentration of metal and chalcogenide ions, pH of the resultant solution, deposition time, temperature, and thickness. Also, the appropriate thermal annealing treatment[15] increases the crystallite size due to the aggregation or coalescence of small nanocrystallites. Also, thermal treatment induced a polymorphic phase transition from a metastable cubic to a stable hexagonal phase. CdSe nanoparticles of spherical and nonspherical shapes, including hexagonal nanorods with the *c*-axis parallel to the surface, nanocubes, nanocables, nanowires, nanoneedles, dendrites, and tetrapods, have been synthesized.[15−17,19−21] These reports were based on CdSe powder synthesized at an elevated temperature (>80 °C), and no structural phase transitions have been reported. A number of researchers[22−24] have reported a phase transformation (β-CdSe → α-CdSe) for chemically synthesized II−VI semiconductors in thin film form with X-ray diffraction (XRD) studies, and no morphological changes have been reported. This is the first successful report on CdSe thin films to clearly show interesting changes in shape and size (morphology) of CdSe nanoparticles during the phase transition from nanocrystalline sphalerite cubic (zinc blende type, β-CdSe) to hexagonal (wurtzite type, α-CdSe) and a band gap shift, as a function of annealing temperature.

2. Experimental Section

2.1. Thin Film Deposition. Cadmium selenide thin films were deposited on glass substrates (7.5 cm × 2.5 cm × 0.1 cm) by the CBD method using analytical grade $Cd(CH_3COO)_2$, 25%, NH_4OH, and freshly prepared sodium selenosulfate (Na_2SeSO_3) solution.[25] All chemicals were purchased from s. d. fine-chem. Ltd. India and used without further purification.

For the deposition of CdSe thin films, 30 mL of 0.5 M $Cd(CH_3COO)_2$ solution was placed in a 100 mL capacity glass beaker, and then ammonia solution was slowly added with constant stirring. Initially, the solution became milky and turbid due to the formation of $Cd(OH)_2$. Further addition of excess ammonia dissolved the turbidity and made the solution clear and transparent. To this, 30 mL of freshly prepared Na_2SeSO_3 solution was added slowly with constant stirring. The resultant pH of the final solution was >12. The solution was stirred for

* Corresponding author. E-mail: rb_kale@yahoo.co.in.
† Rajaram College.
‡ Shivaji University.

10.1021/jp053124c CCC: $30.25
Published on Web 10/06/2005

few seconds and then transferred to another beaker containing cleaned glass substrates inclined vertically at 20° to the wall of beaker. The bath solution was kept at room temperature (300 K) without stirring. The substrates coated with CdSe thin films were removed after 15−18 h, rinsed in double distilled water, and dried in air.

2.2. Characterizations of Thin Films. The CdSe film thickness was measured with the commonly used weight difference method. The crystallographic study was carried out using a Phillips PW-1710 X-ray diffractometer with Cu Kα radiation in the 2θ range from 20° to 100°. The microstructure of the films was studied using a scanning electron microscope (SEM) (Cambridge Stereoscan 259 MK-III). The CdSe films were coated with 100 Å gold−palladium (Au−Pd) layer using a polaron SEM sputter coating unit, before taking the SEM pictures. High-resolution transmission electron microscopic (HR-TEM) analysis was performed with a Philips CM-12 electron microscope (point resolution 2.8 Å) attached to an energy dispersive X-ray analysis (EDAX) analyzer to quantitatively measure the sample stoichiometry. To prepare TEM samples, the CdSe film deposited on glass substrate was scratched and dispersed in alcohol with ultrasonic stirring; then a small drop of suspension was placed on a copper grid covered with a carbon film. To study the optical properties, optical absorption spectra were recorded in the wavelength range 350−850 nm, using a UV−vis−NIR spectrophotometer (Hitachi Model-330, Japan).

3. Results and Discussion

3.1. Reaction Mechanism. The deposition of CdSe thin film takes place when the ionic product (IP) of Cd^{2+} and Se^{2-} ions exceeds the solubility product (SP) of CdSe (i.e., IP ≥ SP (10^{-33})). The CdSe deposition takes place according to the following steps:

Sodium selenosulfate (Na_2SeSO_3) hydrolyzes in solution to give Se^{2-} ions according to

$$Na_2SeSO_3 + OH^- \rightarrow Na_2SO_4 + HSe^- \quad (1)$$

$$HSe- + OH^- \rightarrow H_2O + Se^{2-} \quad (2)$$

Ammonia solution is added in Cd salt solution to form the complex cadmium tetraammine ion [$Cd(NH_3)_4^{2+}$]:

$$Cd^{2+} + 4NH_3 \rightarrow Cd(NH_3)_4^{2+} \quad (3)$$

Then $Cd(NH_3)_4^{2+}$ reacts with Se^{2-} ion to form CdSe thin film:

$$Cd(NH3)_4^{2+} + Se^{2-} \rightarrow CdSe + 4NH_3 \quad (4)$$

3.2. Growth Mechanism. The growth mechanism of thin films in the CBD method can take place either in the bulk of the solution (homogeneous precipitation process) or at the substrate surface (heterogeneous process). Froment and Lincot[26] have proposed that the first process is associated with the agglomeration of colloids formed in the solution by the homogeneous reaction. It can be considered as a "cluster-by-cluster" growth, leading to particulate film. The second process is the growth mechanism involving the reaction of atomic species at the surface; it corresponds to an atom-by-atom process commonly known as an "ion-by-ion" nucleation and growth mechanism. The predominance of one given mechanism is governed by classical laws of homogeneous versus heterogeneous nucleation on a solid surface, involving the supersaturation ratio in the solution and the catalytic activity of the substrate and the rate of stirring.[26] In short, the growth mechanism depends on the experimental conditions.

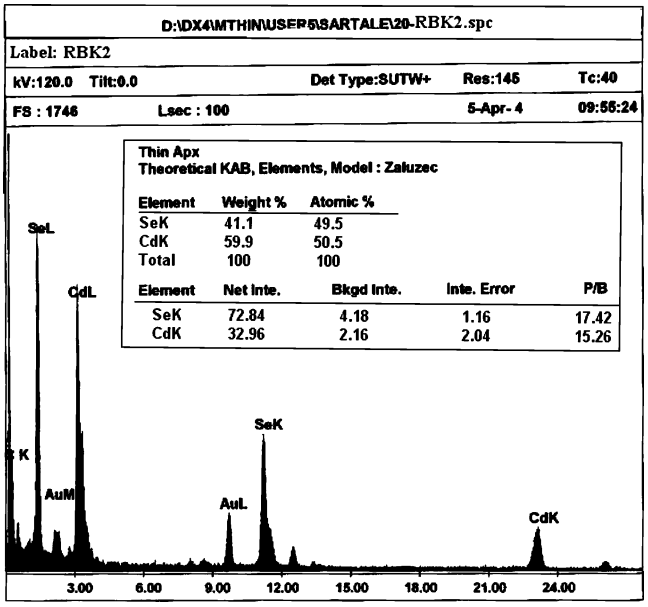

Figure 1. Typical EDAX pattern of as-deposited CdSe film.

In the present study, due to the absence of thermal and mechanical agitation, a strong [$Cd(NH_3)_4^{2+}$] complex, and a stable Na_2SeSO_3 precursor, the Cd^{2+} and Se^{2-} ions were slowly released in the solution, which then condense with an "ion by ion" basis on the substrates that are suitably mounted in the solution.

Chemical bath deposition of semiconductor thin films involves a nucleation/incubation phase followed by a growth phase and terminal phase. Many of the chemically deposited thin films peel off from the substrate at some stage of the growth before reaching terminal thickness. In the present study the film thickness was linearly increased with time, and then saturated (0.23 μm) at 15−18 h deposition time. In present case CdSe films were extremely adherent to the substrate and did not peel off although the deposition was carried out for prolonged time intervals. After a certain time interval or terminal thickness some powdery CdSe material was deposited over the adherent film surface that could be removed with a cotton swab using 2% nitric acid. To study the influence of air annealing on the various film properties, films were annealed in air atmosphere at 373, 473, 573, and 673 K for 4 h.

3.3. Compositional Study. Figure 1 shows a typical EDAX pattern of CdSe film and its relative analysis. The strong peaks for Cd and Se were found in the spectrum, and no impurity peaks were detected in the EDAX spectrum. The carbon peak is due to the dissolved atmospheric CO_2 or carbon-coated grid, and the Au peak was due to gold sputtering on the film surface. The elemental analysis was carried out only for Cd and Se; the average atomic percentage ratio of Cd:Se was 50.5:49.5, showing that the film was in good stoichiometric ratio. The films remained stable up to an annealing temperature of 673 K.

3.4. XRD Study. Cadmium selenide grows either metastable cubic (β-CdSe) or stable hexagonal (α-CdSe) crystal structure. To determine the crystal structure of "as-deposited" and annealed thin films, X-ray diffraction (XRD) patterns were analyzed at room temperature (Figure 2. The XRD pattern of as-deposited CdSe thin film (Figure 2A(a)) was of poor crystallinity, and no well-defined peaks were observed. The peak ((111); d = 3.47 Å)) over a broad hump may correspond to the

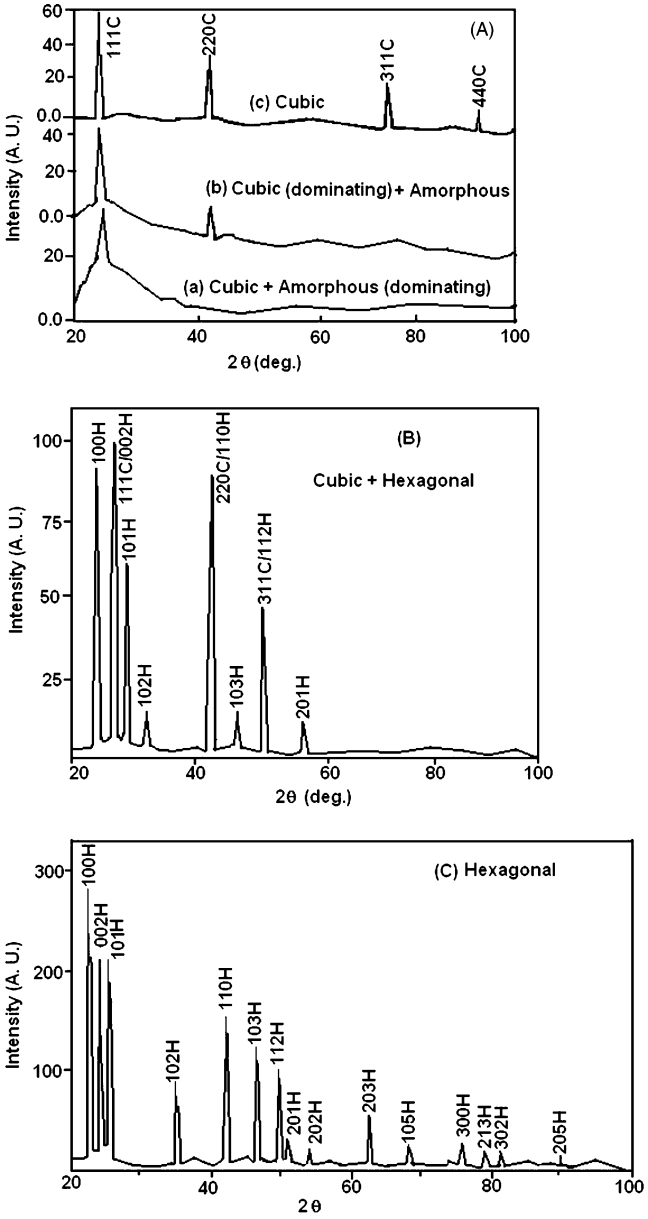

Figure 2. (A) XRD patterns of as-deposited CdSe thin films: (a) as-deposited and annealed at (b) 373 and (c) 473 K. (B) XRD pattern of CdSe thin film annealed at 573 K. (C) XRD pattern of CdSe thin film annealed at 673 K.

sphalerite cubic (zinc blende type) phase of CdSe [JCPDS Card No. 19-191]. The low intensity of the peak confirmed the nanocrystalline nature of sphalerite cubic (zinc blende type) CdSe film. The wide base (broad hump) corresponds to an amorphous phase of CdSe. Thus as-deposited CdSe film has nanocrystalline cubic phase along with amorphous (dominating) phase. Figure 2A(b) shows the XRD pattern of CdSe film annealed at 373 K. A careful analysis of the pattern showed that the broad hump was decreased with the appearance of another peak (002): $d = 2.144$ Å. This clearly indicated the structural change from amorphous (dominating) + nanocrystalline to nanocrystalline cubic along with a small amount of amorphous phase. The XRD pattern of film annealed at 473 K (Figure 2A(c)) clearly shows the polycrystalline nature of the film and the appearance of diffraction peaks of the cubic phase. Also, the XRD peaks were well resolved with considerable improvement in the crystallinity or crystal quality of CdSe film. The comparison of observed *d* values with the standard *d* values and their relative intensities confirmed the formation of the metastable polycrystalline cubic phase of CdSe film. The film annealed at 473 K was preferably oriented along the (111) plane. The film annealed at 573 K (Figure 2B) showed well-defined diffraction cubic peaks along with the appearance of peaks of hexagonal phase. A comparison of observed *d* values and their relative intensities with standard data [JCPDS File Nos. 08-459 and 19-191] confirmed that the major part of β-CdSe phase transforms into α-CdSe phase. Solid state phase transformation typically proceeds via nucleation and growth process. The interface between two contacting β-CdSe (cubic) particles can provide the sites for nucleation of hexagonal phase. Thus, the nucleation rate is determined by the probability of contact between cubic CdSe particles. The film annealed at 673 K is shown in Figure 2C. All the diffraction peaks were indexed to the hexagonal phase of CdSe. The relative intensities of the peaks are in good agreement with standard data [JCPDS File No. 08-459]. However, the positions of peaks were slightly shifted to lower θ values, due to induced tensile strain in CdSe film. This confirmed the total transformation of as-deposited film into stable hexagonal phase. The XRD patterns after thermal annealing showed that the diffraction peaks became sharp with a decrease in the full width at half-maximum (fwhm) due to improvement in crystallization along with the phase transition. It is worthwhile to note that the XRD patterns did not show peaks corresponding to CdO or SeO_2 at any stage of annealing. This clearly confirmed that the CdSe thin films were thermally stable up to annealing temperature 673 K, indicating the high purity of product. It has been proposed that when the materials are in thin film form the transition from cubic to hexagonal crystalline structure reaches its critical point at 573 K.[27] According to Yu and Gielisse,[28] the Gibbs free energy would change toward a lower value, if CdSe goes from the metastable cubic phase to the stable wurtzite phase by the effect of an expansive strain. In this way, the β-CdSe $\rightarrow$ α-CdSe transformation could be considered a first-order phase transition. The occurrence of phase transformation is probably due to the increase in the crystallite size and change in the atomic configuration of CdSe thin films. The temperature for occurrence of phase transformation of sphalerite cubic zinc blende type to hexagonal wurtzite-type structure in CdSe thin films is low (>573 K) compared to the bulk value (for bulk $T \geq 1277$ K),[29] since the smaller nanocrystallite size and the larger surface area that increase the surface-to-volume ratio seem to favor such a phase transformation.[30]

At this point it is necessary to introduce a possible mechanism of β-CdSe $\rightarrow$ α-CdSe phase transformation, proposed by Lozada-Morales et al.,[31] owing to the annealing effect on the phase transformation. In the phase change process, the atoms must go through a potential barrier. Since the cubic phase is the metastable structure of CdSe, and the hexagonal phase is the stable one, in the movement of atoms, due to thermal energy, they pass from a relative minimum to a next lower minimum in the periodic potential. Sullivan[32] has theoretically studied these movements.

Figure 3 illustrates, conventionally, a selenium atom bound to three cadmium atoms as seen along the (111) direction perpendicular to the plane of the page. It is assumed that this isolated molecular representation belongs to the cubic phase of CdSe. The dotted lines represent the relative position of the Cd atoms in a hexagonal structure. A rotation of the three atoms by 60° around the (111) axis will make the full lines, representing the Se−Cd bonds; coinciding with the dotted line, this atom will be placed in an interstitial position with respect to the cubic crystalline structure. In this process, a pair complex

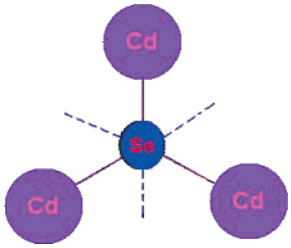

Figure 3. Se atom bound to three Cd atoms as seen from the [111] direction in the β-CdSe lattice. Dotted lines indicate the position of Cd atoms after the rotation of 60° around Se, in order to be in the α-CdSe lattice.

Vcd−*Icd* defect (Frenkel pair) is created. In this way, it can be expected that a lot of interstitial cadmium, with reference to the hexagonal CdSe lattice, should be generated inside the material. Our conclusion is that the recrystallization process occurs more favorably in strained films that are deposited at relatively low temperature. This process consists of the formation of nuclei at regions of high lattice stress or strain, frequently at grain boundaries; and growth of these nuclei, until the old lattice is replaced by a new low stress or strain crystalline structure and finally results in grain growth.[33] If the films were already grown at a relatively high temperature, they already have an energetically favorable orientation and low stress or strain; for this reason they do not recrystallize.

The various structural parameters calculated for CdSe films are given below. The lattice constants *a* for cubic phase structure, and *c* and *a* for the hexagonal phase structure, were determined from the following relations:

$$\text{cubic:} \qquad 1/d^2hkl = (h^2 + k^2 + l^2)/a^2 \tag{5}$$

$$\text{hexagonal:} \qquad 1/d^2hkl = (4/3)\{(h^2 + hk + k^2)/a^2\} + (l^2/c^2) \tag{6}$$

The lattice constants were calculated using observed *d* values of corresponding planes and are listed in Table 1. These parameters were also calculated from standard *d* values. The average lattice constant *a* for cubic phase for as-deposited film was slightly less than the standard value [JCPDS File No. 19-191], indicating that the as-deposited film was under compressive strain. The lattice constants gradually increased with increase in annealing temperature, and lattice parameters acquired the equilibrium values of the bulk when the sample was annealed at 473 K. We conclude that due to the thermal treatment the residual strain present in CdSe quantum dots (QDs) has been relieved. Finally, when the sample was annealed at 573 K and above, calculated lattice parameters were slightly higher than standard (bulk) values, indicating that the annealed films were under tensile strain. This is due to two additive effects as the temperature of sample is increased: strain relief and thermal expansion. The induced change in strain may be responsible for structural phase transformation. Similar strain relief after thermal treatment (up to 673 K) has been reported by Qadri et al.,[34] for chemically synthesized HgS and HgSe powder. The probable explanations of residual strain developed in as-deposited and annealed films can be explained as follows.

During the film deposition and postdeposition treatments, there is always a possibility for the development of strain, which affects the mechanical properties of the film such as the stability of microstructure, the adhesion between film and substrate, and the optoelectronic properties. Strain in the present work is mainly due to the quantum size effect of very small of CdSe QDs and the deposition conditions (low temperature of deposition, high pH of solution, slow deposition rate, etc.), defects that are present in the as-deposited film. If the thin film is deposited free from impurities, the compressive strain is generated at the thin film−substrate interface. The very small crystallites are bonded to the substrate due to surface tension effect and the tensile stress is associated with the coalescence of crystallites, and final grain size is determined by minimization of the sum of the strain energy and surface energy.[35] Also we conclude that, due to the sufficient thickness of films, compressive strain may be generated in the grain boundary model, where the adjacent surfaces of two grains come into contact during the growth without coalescence. In the present case the most probable reasons for the development of tensile strain in the films after annealing are recrystallization, thermal strain, and increase in crystallite size.

1. Recrystallization. The film material recrystallizes after the annealing; as a result of this process, the defects present were annealed out and the average crystallite and/or grain size of the polycrystalline film increases, due to the coalescence of small nanocrystallites that result in the formation of bigger grains. Thus, the recrystallization process gives rise to a densification of the film: transformation of two-dimensional grains into three dimensions, along with changes in atomic configurations and/or orientations, results in a tensile strain contribution.

2. Thermal Strain. Thermal strain appears in the film when the temperature of the film is changed from the deposition temperature. It arises due to the difference in the thermal expansion coefficients of the film and the substrate material.

3. Crystallite Size (D). The average crystallite size was determined using the Debye−Scherrer equation. The average crystallite size was calculated using fwhm's of the (111) and (100) planes for the cubic and hexagonal phases, respectively. For the mixture of both phases, the average of both (111) and (100) planes was considered. Table 1 depicts the calculated values of crystallite sizes of as-deposited and annealed films. From Table 1, it is seen that the average crystallite size was found to be increased with increasing annealed temperature. The improvement in crystallinity of thin films results in the decrease in fwhm of the diffraction peaks. The highest temperature of the present study was 673 K, which is well below the melting point of the CdSe (T_m = 1541 K).[36] Hence it is not expected for the nanocrystallites to undergo melting. However, it is possible that, as the temperature is increased, the surface melting due the dangling bonds may cause recombination of nanocrystallites, hence an increase in the dimensions of the resultant crystallites after annealing.

The possibility for the phase transition is that the cubic structure is the equilibrium phase for CdSe nanoparticles with a free surface. This would be due to surface effects, which can dominate the properties of small particles (∼50% of all the atoms are on the surface of a 40 Å particle). This implies that the structural transition at the elevated temperatures is caused by sintering, since it increases the size; hence the relative influence of the surface decreases so that the bulk, stable hexagonal phase can occur. This mechanism is supported by the observation that the crystal sizes of CdSe QDs at which structural phase transition occurs are about 12 nm. The importance of surface effects is demonstrated by the mixed cubic and hexagonal seen, thought to be the result of mismatch-induced strain expansion between the CdSe and the substrate.

3.5. Morphological Study. From morphological observations, one can get valuable information regarding the growth mechanism, shape and size of nanoparticles and/or grains, and phase of materials and its transformations that occur during the thermal

TABLE 1: Phase, Lattice Parameters, Crystallite Size, Band Gap, and Residual Strain for As-Deposited and Annealed CdSe Thin Films

		lattice parameter (Å)				
thin film	phase	*c*	*a*	crystallite size *D* (nm)	band gap E_g (eV)	residual strain $\epsilon \times 10^{-3}$
AD[a]	cubic		6.01	4	2.3	1.428
373 K	cubic		6.045	6	2.0	0.812
473 K	cubic		6.084	8	1.8	0.085
573 K	cubic		6.084	12	1.7	−0.256
573 K	hexagonal	7.021	4.308	12	1.7	−0.256
673 K	hexagonal	7.032	4.310	18	1.7	−1.362

[a] AD, as-deposited.

annealing. The as-deposited CdSe film did not show well-resolved XRD peaks. Therefore, to confirm the nanoparticle size and shape of grains, the as-deposited film was analyzed with scanning electron microscopy (SEM) and transmission electron microscopy (TEM). Figure 4a shows the SEM image of as-deposited CdSe thin film. From SEM, it was observed that as-deposited thin films are smooth, uniform, homogeneous, well covered to the substrate surface, densely packed, and without any cracks, voids, or pinholes. SEM also shows fine CdSe nanoparticles distributed within an amorphous matrix. High-resolution TEM (HR-TEM) (Figure 4b) clearly shows that the film consists of randomly oriented small CdSe nanocrystallites of ca. 4 nm diameter (in agreement with XRD), distributed within a continuous (amorphous) matrix. Thus, it clearly demonstrates that the CdSe film consists of a mixture of nanocrystalline phase along with some amorphous phase with the same stoichiometry. The amorphous phase has a "gluelike" function that holds CdSe nanoparticles together. The selective area electron diffraction (SAED) pattern (Figure 4c) shows one sharp and continuous diffraction ring pattern that corresponds to the (111) ($d = 3.51$ Å) plane of cubic nanocrystalline CdSe material. The broad and diffuse ring pattern may be due to an amorphous matrix present in as-deposited CdSe film. Figure 4c also shows the Fourier transformation (FT), which gave a lattice spacing of 3.51 Å that corresponds to the (111) plane of the cubic phase (the inset shows the reference used for it). Also, morphological studies confirmed that the deposition took place via heterogeneous nucleation, i.e., ion-by-ion mechanism, due to the aggregation of particles on the surface of substrate without coalescence.

The annealed CdSe films showed well-resolved XRD peaks and information regarding the crystal structure; therefore, the surface morphology of annealed films was obtained with SEM. The SEM (Figure 5A) of film annealed at 373 K shows the spherical nanoparticles, over which some amorphous phase is clearly seen, indicating improvement in the crystallinity. Thus it clearly shows that, due to thermal annealing, the particles try to coalesce and/or diffuse together to form nanosized spherical grains that change the amorphous phase of as-deposited film into nanocrystalline cubic phase. The SEM (Figure 5B) of CdSe thin film annealed at 473 K shows a remarkable change in surface morphology, i.e., growth of large spherical CdSe nanoparticles (diameter $\sim$ 400−600 nm), due to coalescence and/or diffusion of a number of small CdSe nanoparticles due to thermal energy. During nucleation, due to the thermal annealing process, the surface energy contribution dominates, so that reductions in the free surface area and surface energy would be favored. The free surface area can be minimized by the nucleus adopting a spherical shape (minimum surface-to-volume ratio). This can be achieved by adopting a crystal structure amenable to the formation of a spherelike nucleus by exposing close-packed low-energy planes as facets on the surface of the nucleus. A symmetry consideration favors the cubic structure over the hexagonal one, resulting in the formation of a spherical nucleus with a large number of [111] facets on the surface. Therefore, CdSe nanoparticles adopt a cubic

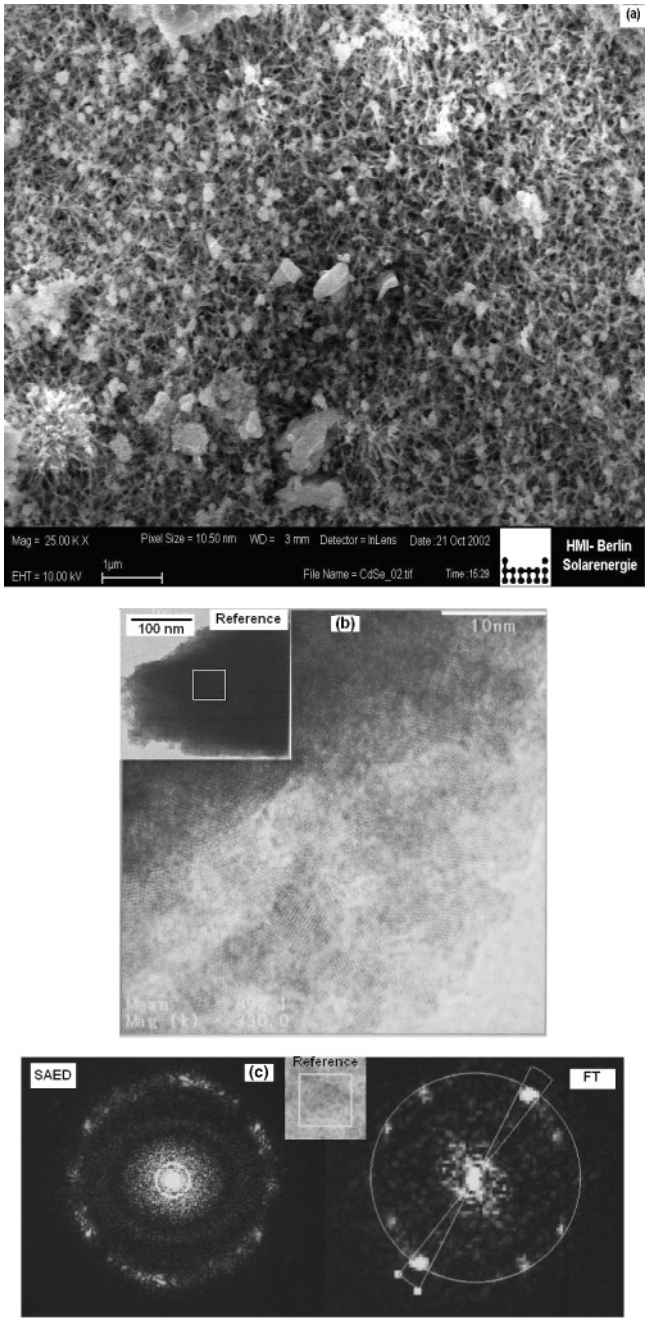

Figure 4. (a) SEM of as-deposited CdSe thin film. (b) HR-TEM of as-deposited CdSe thin film. (Inset shows TEM region used for it.) (c) SAED and FT of as-deposited CdSe thin film. (Inset shows reference used for it.)

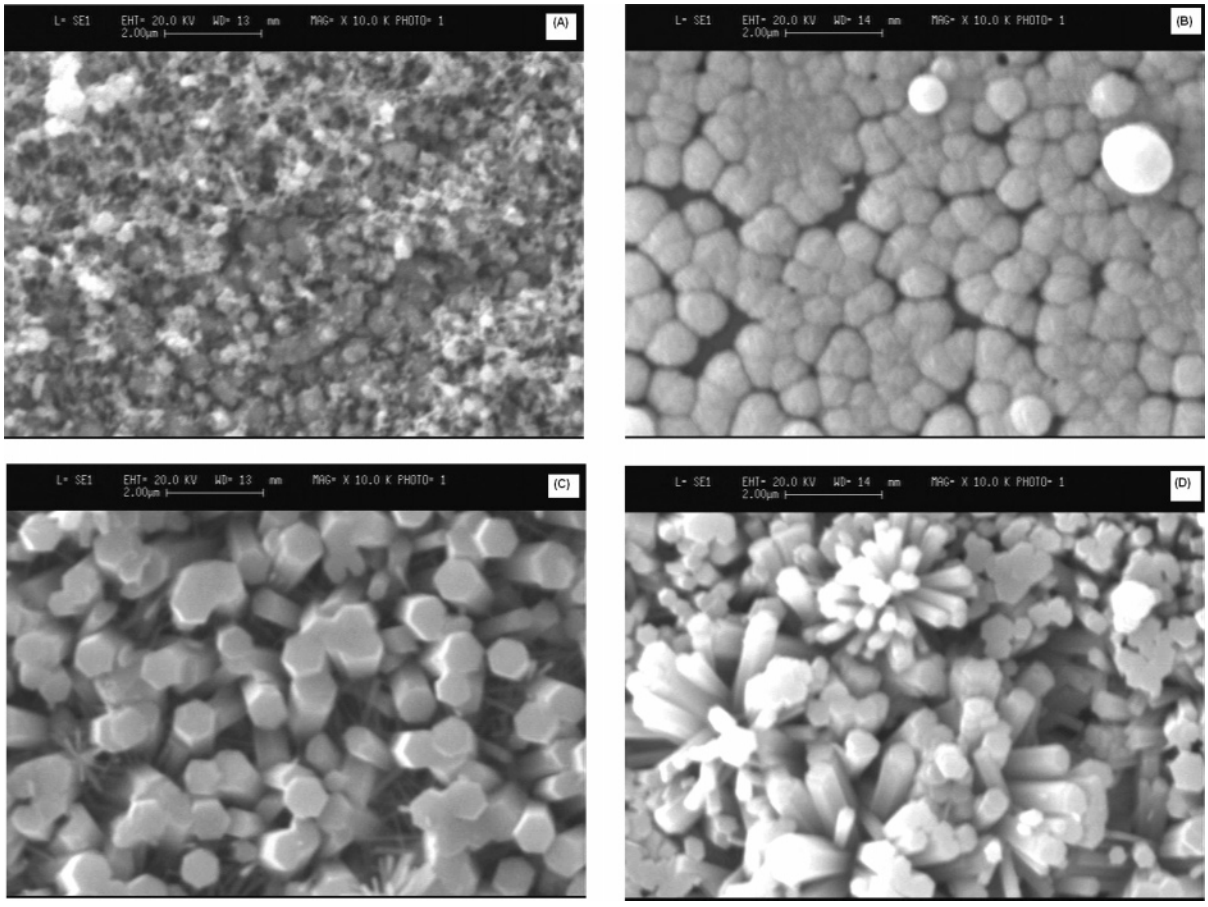

Figure 5. (A) SEM of CdSe thin film annealed at 373 K. (B) SEM of CdSe thin film annealed at 473 K. (C) SEM of CdSe thin film annealed at 573 K. (D) SEM of CdSe thin film annealed at 673 K.

structure at the initial stage of annealing. The SEM (Figure 5C) of film annealed at 573 K clearly shows two types of structural behaviors: one is elongated columnar nanorods of diameter ~ 250 nm and length ~ 1 μm (having a separate existence and some are interdiffused with each other) with the *c*-axis perpendicular to the substrate surface, indicating the hexagonal phase and nanowires parallel to the surface of thin films that corresponds to the cubic phase of CdSe. It was confirmed that, when CdSe thin film was annealed at 573 K, metastable cubic (β-CdSe) phase was partially transformed into stable hexagonal (α-CdSe) phase that resulted in the mixture of β-CdSe and α-CdSe phases called the polytype structure. The SEM (Figure 5D) of CdSe thin film annealed at 673 K shows the total conversion of nanowires into three-dimensionally grown elongated columnar nanorods (diameter ~ 200 nm and length ~ 2 μm) that are strongly oriented in the plane perpendicular to the substrate surface. They were united at the base, and showed a separate existence when they came out from the surface. They formed a cauliflower-like structure, originating from the substrate. The thermal energy provides kinetic force for the anisotropic development of columnar nanorods with a unique *c*-axis orientation corresponding to the most stable hexagonal (α-CdSe) crystal structure. The increase in surface area, due to the change in spherical, bigger nanoparticles of cubic phase and six regular faces of columnar nanorods of hexagonal phase, is beneficial for gas sensors and optoelectronic devices.

We studied the effects of various parameters such as recrystallization, increase in crystallite and grain growth, change in lattice parameters, and change in colors of CdSe films after annealing, since these parameters affect the optical properties of films.[30] The transmission spectra of CdSe films were studied

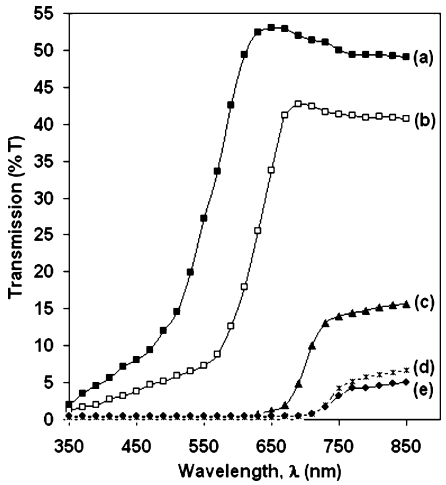

Figure 6. Plots of optical transmission (% *T*) vs wavelength for CdSe thin films: (a) as-deposited and annealed at (b) 373, (c) 473, (d) 573, and (e) 673 K.

in the wavelength range 350−850 nm. Figure 6 shows the variation of optical transmission (% *T*) with the wavelength (λ) of as-deposited and annealed CdSe thin films. It shows a decrease in optical transmission with increasing annealed temperature of CdSe thin films. It is clearly seen that the as-deposited film showed a blue shift in the transmission spectra. The transmission edge was shifted to the longer wavelength with increasing annealing temperature of CdSe film (i.e., CdSe films showed red shifts in their optical spectra after annealing). It may be due to the increase in crystallite size, lattice parameters, and change in color of CdSe films, from red orange

to red to dark brown and finally into dark black, that resulted in the decrease in transmission spectra; consequently, CdSe films showed red shifts in their optical spectra.

The band gaps E_g's of CdSe as-deposited and annealed films were found from the plots of $(\alpha h\nu)^2$ versus $h\nu$, and are listed in Table 1. The E_g for as-deposited CdSe thin film was found to be 2.3 eV, which showed a 0.6 eV blue shift from the standard band gap value of bulk material. A number of workers[1,2,37,38] have reported blue shifts in the optical spectra for chemically deposited CdSe, ZnS, and PbSe materials. Such a higher value of band gap energy is most probably due to a size quantization effect in CdSe QDs that leads to a series of discrete states in the conduction and valence bands, resulting in the increase of the effective band gap. The E_g continuously decreased with increasing annealing temperature and reached the standard bulk value ($E_g = 1.7$ eV) at 573 K. Since crystallite size was increased with increase in annealing temperature, due to sintering of small nanocrystallites into effectively larger crystallites, a loss of quantum size effect resulted. The larger crystallite size with low transmission of stable hexagonal structure has special applications in photoelectrochemistry (PEC) and photovoltaic cells.

4. Conclusions

CdSe thin films were deposited from aqueous alkaline solution using the CBD method. The films were grown with nanocrystalline cubic structure with a diameter of 4 nm along with amorphous phase, and the crystallite size was varied to values near that of the bulk by subsequent annealing. Thermal annealing also causes the structural transformation from the cubic to the hexagonal structure of bulk CdSe. The cubic structure may be due to metastability or an equilibrium surface effect. Also, there is a correlation between CdSe nanocrystallites and crystal structure, indicating that a minimum crystallite size is required for the formation of the stable (bulk) hexagonal crystal structure. Increase in crystallite size and the recrystallization process that took place resulted in the decrease in band gap E_g of CdSe films, in accordance with quantum confinement effect. The CBD method is simple and convenient and provides a new way to fabricate other nanosized semiconductor compounds and a suitable route to study the effect of thermal treatment on crystallite size, phase transition, and changes in morphological and optoelectronic properties.

Acknowledgment. R.B. Kale is grateful to Dr. S.N. Pathan, Director of Higher Education, Maharashtra and Dr. (Mrs.) V.M. Kurane, Principal of Rajaram College, Kolhapur for encouragement and constant support to carry out the research work.

References and Notes

(1) Zhang, Y.; Li, Y. *J. Phys. Chem. B* **2004**, *108*, 17805.
(2) Zhu, J.; Palchik, O.; Chen, S.; Gedanken, A. *J. Phys. Chem. B* **2000**, *104*, 7344.
(3) Coe, S.; Woo, W. K.; Bawendi, M. G.; Bulvoc, V. *Nature* **2002**, *420*, 800.
(4) Gorer, S.; Hodes, G. *J. Phys. Chem.* **1994**, *98*, 5338.
(5) Empedocles, S. A. *J. Phys. Chem. B* **1999**, *103*, 1826.
(6) Ludolph, B.; Malik, M. A.; Brien, P. O.; Revaprasadu, N. *Chem. Commun.* **1998**, *18*, 1849.
(7) Sharma, K. C.; Sharma, R.; Garg, J. C. *Jpn. J. Appl. Phys.* **1992**, *31*, 742.
(8) Gutierrez, M. T.; Ortega, J. *J. Electrochem. Soc.* **1989**, *136*, 2316.
(9) Bouroushian, M.; Loizos, Z.; Syrellis, N.; Maurin, G. *Thin Solid Films* **1993**, *10*, 229.
(10) Shaw, G. A.; Parkin, I. P. *Inorg. Chem.* **2001**, *40*, 6940.
(11) Garcia, V. M.; Nair, M. T. S.; Nair, P. K.; Zingaro, R. A. *Semicond. Sci. Technol.* **1996**, *11*, 427.
(12) Cachet, H.; Essaaidi, H.; Froment, M.; Maurin, G. *J. Electroanal. Chem.* **1995**, *396*, 175.
(13) Yochelis, S.; Hodes, G. *Chem. Mater.* **2004**, *16*, 2740.
(14) Rincon, M. E.; Jimenez, A.; Orihuela, A.; Martinez, G. *Sol. Energy Mater. Sol. Cells* **2001**, *70*, 163.
(15) Palchik, O.; Kerner, R.; Gedanken, A.; Weiss, A. M.; Slikin, M. A.; Palchik, V. *J. Mater. Chem.* **2001**, *11*, 874.
(16) Crouch, D. J.; Brien, P. O.; Malik, M. A.; Skabara, P. J.; Wright, S. P. *Chem. Commun.* **2003**, *24*, 1454.
(17) Nair, P. S.; Fritz, K. P.; Scholes, G. D. *Chem. Commun.* **2004**, *24*, 2084.
(18) Gutierrez, M. T.; Salvador, P. *Sol. Energy Mater.* **1987**, *15*, 99.
(19) Rao, C. N. R.; Govindaraj, A.; Deepak, F. L.; Gunari, N. A. *Appl. Phys. Lett.* **2001**, *78*, 1853.
(20) Peng, Q.; Dong, Y.; Li, Y. *Inorg. Chem.* **2002**, *41*, 5249.
(21) Urbieta, A.; Fernadez, P.; Piqures, J. *Appl. Phys. Lett.* **2004**, *85*, 5968.
(22) Zelaya-Angel, O.; Alvarado-Gil, J.; Lozada-Morales, R.; Vargas, H.; Ferreira da Silva, A. *Appl. Phys. Lett.* **1994**, *64*, 291.
(23) Bandaranayake, R. J.; Wen, G. W.; Lin, J. Y.; Jiang, H. X.; Sorensen, C. M. *Appl. Phys. Lett.* **1995**, *67*, 831.
(24) Huang, F.; Banfield, J. F. *J. Am. Chem. Soc.* **2005**, *127*, 4523.
(25) Kale, R. B.; Lokhande, C. D. *Semicond. Sci. Technol.* **2005**, *20*, 1.
(26) Froment, M.; Lincot, D. *Electrochim. Acta* **1995**, *40*, 1293.
(27) Zelaya, O.; Alvarado-Gil, J. J.; Lozada-Morales, R.; Vargas, H.; Ferreira da Silva, A. *Appl. Phys. Lett.* **1994**, *64*, 291.
(28) Yu, W. C.; Gielisse, P. *Mater. Res. Bull.* **1971**, *6*, 621.
(29) Rao, C. N. R.; Rao, K. J. *Phase Transitions in Solids: An Approach to the Study of the Chemistry and Physics of Solids*; McGraw-Hill: New York, 1976; p 285.
(30) Yoganaranrasimhan, S. R.; Rao, C. N. R. *Trans. Faraday Soc.* **1962**, *58*, 476.
(31) Lozada-Morales, R.; Zelaya-Angel, O.; Torres-Delgado, G. *Appl. Phys. A* **2001**, *73*, 61.
(32) Sullivan, J. L. *IEEE Trans. Sonics Ultrason.* **1985**, *32*, 71.
(33) Reed-Hill, R. E. *Physical Metallurgy Principles*; PWS Publishers: Boston, MA, 1973; p 284.
(34) Qadri, S. B.; Kuno, M.; Feng, C. R.; Rath, B. B.; Yousuf, M. *Appl. Phys. Lett.* **2003**, *83*, 4011.
(35) Puiso, J.; Tamulevicius, T.; Laukaitis, G.; Lindroos, S.; Leskela, M.; Snitka, V. *Thin Solid Films* **2002**, *403*, 457.
(36) Tybulewicz, A. *Semiconducting II-VI and V-VI Compounds*; Plenum Press: New York, 1969.
(37) Gorer, S.; Albu-Yaron, A.; Hodes, G. *J. Phys. Chem.* **1995**, *99*, 16442.
(38) Hu, P.; Liu, Y.; Fu, L.; Cao, L.; Zhu, D. *J. Phys. Chem. B* **2004**, *108*, 936.